Falling Film Heat Transfer Analysis on a Bank of Horizontal Tube Evaporator

Heat transfer analysis of falling film evaporation on a bank of horizontal tubes is investigated in this study. Liquid falling from one tube to the next lower one is considered as a thin liquid jet impinging on the top of the tube with a uniform free falling velocity. The hydrodynamic and thermal solutions are obtained by a finite difference method. In these solutions the heat transfer coefficients are modified to account for waviness.

Liquid film thickness and local and average heat transfer coefficients are obtained for the constant heat flux and isothermal boundary conditions. Convective heat transfer effects are shown to be dominant as Peclet number increases. Heat transfer coefficients for the tubes in a tube bank decrease from the first tube onwards until the fully developed region is reached. The present predictions agree favorably with the reported heat transfer data.

G. Kocamustafaogullari and I. Y. Chen
Department of Mechanical Engineering
University of Wisconsin
Milwaukee, WI 53201

Introduction

Horizontal tube evaporators, where condensation takes place inside horizontal tube while an evaporating film flows over the outside of the tube banks, are extensively utilized in desalination, chemical process industries, and have recently been proposed in ocean thermal energy conversion systems. Such heat exchangers are characterized by high heat transfer coefficients at low feed rates and small temperature differences. Despite the importance of horizontal tube evaporators, information for predicting their heat transfer performance is still limited. As indicated by Newson (1978), Moalem and Sideman (1976), and Fletcher et al. (1973), the evaporating liquid film heat transfer coefficient is the governing parameter in the overall heat transfer coefficient for horizontal tube evaporators. Evaluation of the heat transfer performance of horizontal tube evaporators is, therefore, best achieved by a reliable predictive method for the evaporation side heat transfer coefficients. It is the aim of this study to analyze evaporation heat transfer for liquid films flowing across horizontal tubes set into a vertical in line array.

Prior experimental studies on evaporation heat transfer data for horizontal evaporators were primarily sponsored by the Office of Saline Water. Based on the Office of the Saline Water experimental reports, some of which are listed in the Literature Cited section, Newson (1978) offered analysis to link the process variables to the heat transfer coefficients in horizontal evaporators, but no analytical or empirical methods was presented. Over the last decade, horizontal tube evaporators were proposed for use in Ocean Thermal Energy Conversion System (OTEC). In support of this development, a number of tests were conducted on horizontal tubes by Sabin and Poppendiek (1978), Owens (1978) and Conti (1978). For the thermal design of OTEC heat exchangers, Owens (1978) presented a correlation which was empirically obtained from his ammonia data and Liu's (1975) water data to predict the evaporation heat transfer coefficients on horizontal tubes. Lorenz and Yung (1978, 1979) also proposed a simple model for predicting film evaporation heat transfer coefficients on a horizontal tube bundle. This model combined correlations for the thermally developing region at the top tubes and the fully developed region at the lower tubes in a tube bundle. Lorenz and Yung's predictions were shown to have good agreement with ammonia and water data of Fletcher et al. (1973, 1975), Owens (1978), Sabin (1978), Conti (1978), and Liu (1975).

Although few heat transfer analyses on a single horizontal tube evaporator or on a tube banks have been published, film evaporation on a horizontal tube was experimentally and theoretically studied by a number of workers to gain an understanding of heat transfer characteristics of films flowing over horizontal tubes. Fletcher et al. (1973, 1975) experimentally investigated film evaporation on a heated tube. Heat transfer coefficients at various liquid flow rates, heat flux, and saturation

Present address of I. Y. Chen: Sundstrand Advanced Technology Group, Rockford, IL 61125.

temperatures were reported for water and brine. Solan and Zfati (1974) conducted an experimental study with subcooled liquid film, flowing over a horizontal tube at film Reynolds number in the range of 100–700. They also presented an analytical method to calculate the local heat transfer coefficient in the thermally developing and fully developed regions. Their results for laminar film flow were in good agreement with the experimental data for film Reynolds number up to 600. Parken (1975) and Parken and Fletcher (1982) investigated film evaporation on a horizontal tube. Their laminar analysis involved an integral method and a finite difference scheme. Analytical results were found to have in good agreement with their data. Liu (1975) also conducted an experimental study to simulate liquid falling on a tube bundle. The heat transfer data were obtained for various separation distances between the top of the test tube and the bottom of the feeding tube. Heat transfer predictions were obtained numerically for different laminar and turbulent models; the turbulent model was shown to have better agreement with the test data.

Moalem and Sideman (1976) presented a laminar analysis to solve the local heat transfer coefficients of the interacting condensation and evaporation processes inside and outside a horizonal evaporator tube. Their study was extended by Moalem and Sideman (1977) to conduits with an elliptical cross section. Comparison of the heat transfer predictions with the experimental data of Sideman and Moalem (1976) indicated the laminar theory yielded lower predictions at $Re > 150$. The deviation was attributed to wave action of wave at the film surface. Thus, a correction factor empirically obtained by Zazuli (1959) was added to the laminar solution to account for the wavy effect. More recently, the film flow analyses on horizontal tubes was applied to the cooling of Calandria tubes in certain nuclear reactors for cases of accidents involving the loss of coolant in certain nuclear power reactors. Rogers (1981) also proposed a laminar analysis which is similar to that of Solan and Zfati (1974). Here a correction factor for interfacial waviness, which had been originally suggested by Kutateladze (1979), was added to improve the heat transfer predictions.

As indicated by the brief survey the heat transfer problem for evaporating lilquid films flowing across a tube bundle has not been fully explored. In addition, between-tube evaporation, Lorenz and Yung (1978), as well as tube spacing, Lin (1975), Danilova et al. (1976) and Chyu and Bergles (1987), both of which affect the heat transfer behavior of an entire tube bank, is not yet fully understood. It is the purpose of this study to analyze the evaporating film heat transfer coefficients from tube to tube in a vertical tube bank of horizontal evaporators. The effects of various factors which influence heat transfer rates, such as tube diameter, film flow rate, operating temperature, between-tube spacing, and tube location within tube bundle, are also investigated.

Analysis

Physical model

When a liquid film is flowing on a vertical row of horizontal tubes, basically three different flow patterns of liquid flow between the adjacent tubes can be observed: droplet dripping, liquid columns, and liquid sheets, Moalem et al. (1978, 1979), Sideman et al. (1978), Yung et al. (1980), Dhir and Taghavi (1981), and Mitrovic (1986). These three distinctive flow patterns are illustrated in Figure 1. Which of these flow patterns

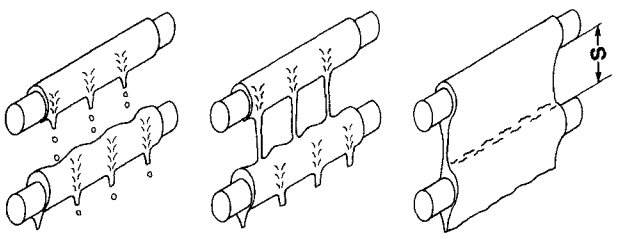

Figure 1. Patterns of liquid flow between two adjacent horizontal tubes (Mitrovic, 1986): a. droplet drippling; b. liquid columns; and c. liquid sheets.

can be expected in an actual case depends mainly on the flow rate, the tube spacing, and the physical properties of the liquid. The droplet dripping, Figure 1a, usually appears for a lower flow rate and a larger tube spacing. This flow-pattern changes at first to that shown in Figure 1b, and then to the pattern 1c when the flow rate increases and/or the tube spacing decreases.

Transport characteristics of films flowing over horizontal tubes strongly depend on the existing flow pattern. Although we do not have well-established flow pattern transition criteria that can be used to predict transition boundaries in terms of characteristic parameters, such as flow rate, tube spacing, and fluid properties, experimental observations of Moalem et al. (1978), Ganic and Roppo (1980), and Mitrovic (1986) indicate that the transition between dripping and liquid columns occurs at $Re \simeq 150 - 200$, whereas the transition from liquid columns to continuous liquid sheet occurs at $Re \simeq 315 - 600$. The transition Re number range was affected by tube spacing and liquid properties which were different in these experiments. As experimentally demonstrated by Sideman et al. (1978), at relatively high Reynolds numbers, $Re \geq 600$, the film flow characteristics around the tube were independent of whether the feed on top of the tube arrives as a continuous film or as continuous columns. Since the typical operating range of horizontal tube evaporators is generally kept in the range of film Reynolds number greater than about 800, it is conservative to model the flow pattern between two horizontal tubes as a continuous sheet, Figure 1c. The following analysis deals with the case where the liquid between the tubes is a smooth continuous film. Therefore, the results cannot be used for low-Reynolds number flows where the droplet dripping flow pattern dominates.

The present analysis considers liquid falling on a heated horizontal tube bank. It is assumed that there is no nucleate boiling in the film and that only surface evaporation occurs. The physical system is illustrated in Figure 2. In the absence of vapor crossflow, saturated liquid at T_v and an initial flow rate of $2\Gamma_o$ falls as a continuous sheet, impinging on the first tube of a tube bank. Thus, the heat transfer behavior of the first tube is similar to that of a single heated tube subject to a sheet of falling liquid. The liquid film flows tangentially in the arc length direction along the tube periphery. It drains down to the bottom of the tubes and falls on the top of the next lower tubes ($x = 0$) under the influence of gravity.

For horizontal tube evaporators, the liquid wetting rate is generally kept in the range of film Reynolds number between 800 and 4,000 which results in the flow being either wavy laminar or just slightly turbulent. This range of Reynolds number for

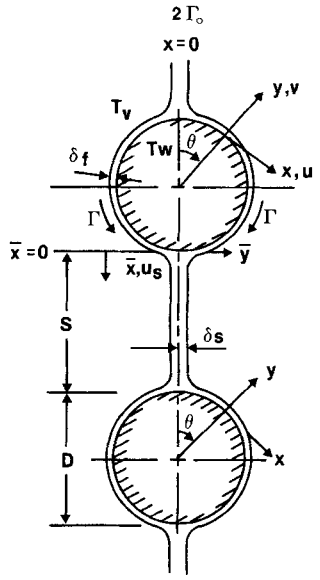

Figure 2. Modeling of liquid film falling on horizontal tubes in a tube bank.

a laminar treatment may contradict common knowledge that for a liquid film flow on a vertical surface, the transition from laminar to turbulent flow is generally considered to occur in the range of film Reynolds numbers between 1000 and 2000, Seban (1978), Kutateladze and Gogonin (1979), Fujita and Veda (1978), and Rogers (1981). These observations, however, are not directly applicable for liquid film flow on a horizontal pipe since the flow is neither fully developed nor in a constant vertical application. The flow on a horizontal pipe can be approximated by the flow on inclined surfaces, for which Ueda and Tanaka's (1975) measurements indicate that the liquid film as a whole are much more laminar-like than turbulent in a range of film Reynolds numbers up to the experimental limit of 6,000. Parken (1975) also observed that laminar film flow on a horizontal pipe can be maintained at the film Reynolds number as high as 6,044. In view of the above discussion, a laminar flow model is assumed and the heat transfer coefficients are then corrected for waviness.

Since liquid falling to the next lower tubes has been heated by the upper tubes, the local flow rate and temperature profile reaching the top of the next tube will change from tube to tube in multiple tube array. Therefore, hydrodynamic and thermal field equations associated with: a) a liquid film flowing over horizontal tubes; (b) the liquid sheet falling between tubes; and c) the stagnation point boundary layer solution at the top of the tubes must be simultaneously solved to obtain heat transfer predictions for the whole tube bank. Formulation and solution techniques for these three problems are illustrated below.

Governing equations for film flowing over horizontal tubes

Assuming that the film thickness, δ_f is small compared to the tube diameter, D, the curvature effect may be neglected. The field equations governing the kinematic, dynamic and energetic fields of the flow can be simplified by using the thin film approximation as introduced by Kocamustafaogullari (1985) and Chen (1984). The Reynolds number, assumed to be in the range of 800 to 4,000, allows the inertia terms to be the same magnitude as the viscous and gravity terms in the momentum equation, and the convective heat transfer terms have the same order as the conductive heat transfer terms. The effects of interfacial shear stress, pressure gradient and surface tension on the circumferential film over the tubes are assumed to be small and, hence, neglected. The simplified governing equations for an incompressible fluid are given in Chen (1984). In dimensionless form they are given as follows:

Continuity Equation

$$\frac{\partial u'}{\partial x'} + \frac{\partial v'}{\partial y'} = 0 \tag{1}$$

Momentum Equation

$$u'\frac{\partial u'}{\partial x'} + v'\frac{\partial u'}{\partial y'} = \left(\frac{8}{Re^2}D'\right)\sin x' + \left(\frac{2}{Re}\frac{D'}{\delta'^2}\right)\frac{\partial^2 u'}{\partial y'^2} \tag{2}$$

Energy Equation

$$u'\frac{\partial T'}{\partial x'} + v'\frac{\partial T'}{\partial y'} = \left(\frac{2}{Pe}\frac{D'}{\delta'^2}\right)\frac{\partial^2 T'}{\partial y'^2} \tag{3}$$

To complete the formulation, the following dimensionless boundary conditions are introduced

$$\text{at } y' = 0,\ x' \geq 0; \quad u' = 0,\ v' = 0$$
$$\text{either } T' = 1 \quad \text{(isothermal condition)}$$
$$\text{or } \frac{\partial T'}{\partial y'} = -\delta' \quad \text{(constant heat flux)} \tag{4}$$

$$\text{at } y' = 1,\ x' \geq 0; \quad \frac{\partial u'}{\partial y'} = 0; \quad T' = 0 \tag{5}$$

$$\text{at } x = 0,\ y' > 0; \quad u' = u'_o,\ v' = v'_o$$
$$T' = 0 \quad \text{(at the top tube)}$$
$$T' = T'(y') \quad \text{(at the lower tubes)} \tag{6}$$

where u'_o and v'_o are the dimensionless initial velocity profiles at the top of the tube. The initial temperature profile $T'(y')$ at the top of the lower tubes, e.g., at $x' = 0$, is calculated for a liquid film falling between the tubes. In Eqs. 1 through 6, the dimensionless variables are defined as follows:

$$x' \equiv x/R,\ 0 < x'(=\theta) < \pi; \quad y' \equiv y/\delta_f,\ 0 < y' < 1$$
$$u' \equiv u/u_f; \quad v' \equiv v/(u_f \delta_f/R)$$
$$D' \equiv D/L_c; \quad S' \equiv 2S/L_c; \quad \delta' \equiv \delta_f/L_c \tag{7}$$

$$\text{either } T' \equiv (T - T_v)/(T_w - T_v) \quad \text{(isothermal condition)}$$
$$\text{or } T' \equiv (T - T_v)/(q''_w L_c/k) \quad \text{(constant heat flux)}$$

where the characteristic film thickness, L_c, and the reference velocity, u_f, are defined as

$$L_c \equiv (\nu^2/g)^{1/3} \tag{8}$$

$$u_f \equiv \frac{\Gamma}{\rho L_c} = \frac{Re\nu}{4L_c} \tag{9}$$

In these equations the liquid mass flow rate flowing over one side of the tube, Γ, is expressed as

$$\Gamma = \rho \int_0^{\delta_f} u\, dy = \rho\delta_f \int_0^1 u\, d(y/\delta_f) \tag{10}$$

Thus, the local film thickness, δ_f, is given by

$$\delta_f = \Gamma/\rho \int_0 u\, d(y/\delta_f) \tag{11}$$

which, in dimensionless form, becomes

$$\delta' = 1 \Big/ \int_0^1 u'\, dy' \tag{12}$$

This problem is a boundary value problem with four governing equations (Eqs. 1, 2, 3 and 12), and four unknowns, u', v', T' and δ', and boundary conditions specified by Eqs. 4, 5, 6. The starting values of u'_o, v'_o, and δ'_o at the top of the tubes can be obtained by using a stagnation point boundary layer solution. The detailed analysis of the stagnation point solution is discussed later. The local film thickness, velocity and temperature profiles around the tubes are then solved by using a finite difference method. The method of solution used follows Schlichting's (1979) finite difference procedure for solving nonlinear partial differential equations. The partial differential terms in the y' direction are replaced by the central difference forms. On the other hand a backward difference formula is used for the partial derivatives in the x' direction. The details of the solution procedure were described by Chen (1984). The accuracy of the finite difference solution depends on the grid size used in the calculation. For a relatively small number of mesh points, the results show oscillation around the converging solution. After some numerical testing, the forward step size was set equal to 180 steps from the top to the bottom of the tube, and the grid spacing in the film direction was equally divided into 20 strips.

Governing equations for liquid sheet falling between the tubes

Here it may be assumed that the liquid velocity at the bottom of the upper tube is negligible, and that the liquid has no initial velocity as it falls down. Therefore, the liquid velocity at any position between the upper and lower tubes, Figure 1, is given by the free fall expression

$$u_s = (2g\bar{x})^{0.5} \tag{13}$$

Further, the liquid films draining from the tube sides are assumed to be well mixed as the liquid flows from two sides and the films coalesce at the bottom of the tube. Hence, a uniform bulk mean temperature of liquid may be assumed which is determined from the temperature profiles of liquid films at the bottom of the upper tube. This uniform temperature is then used as the initial temperature profile of the falling liquid as it departs the tube. The liquid descends vertically as a continuous sheet with mass flow rate 2Γ, and its local width $2\delta_s$ can be expressed as

$$2\delta_s = \frac{2\Gamma}{\rho u_s} = \frac{2\Gamma}{\rho(2g\bar{x})^{0.5}} \tag{14}$$

Since a small portion of the falling liquid is evaporated from each tube, the local mass flow rate leaving the upper tube is used in Eq. 19 that results in

$$2\Gamma_{n+1} = 2\Gamma_n - \frac{\pi D\bar{h}_n}{h_{fg}}(T_w - T_v) \quad \text{(isothermal condition)}$$

$$2\Gamma_{n+1} = 2\Gamma_n - \frac{\pi D q''_w}{h_{fg}} \quad \text{(constant heat flux)} \tag{15}$$

where the subscript n identifies the nth tube within the tube bank, and $\bar{h}_n$ is the average heat transfer coefficient for the nth tube.

A thermal analysis of the liquid film falling between the tubes leads to the temperature profile for the liquid sheet between two tubes. Consequently, the temperature distribution of the falling liquid sheet, before reaching the top of the next lower tube, is used as the initial temperature profile at $x = 0$ of the tube.

Since the liquid flow is only in the vertical direction, the dimensionless energy equation for falling liquid flow between the tubes is then given as

$$\frac{\partial T''}{\partial x''} = \left(\frac{8}{PrRe}\right) S''^{1.5} \times {}''^{0.5} \frac{\partial^2 T''}{\partial y''^2} \tag{16}$$

with the dimensionless boundary conditions

$$\frac{\partial T''}{\partial y''} = 0 \quad \text{at } y'' = 0,\ x'' > 0$$

$$T'' = 0 \quad \text{at } y'' = 1,\ x'' > 0$$

$$T'' = T''_m \quad \text{at } y'' = 0,\ x'' = 0 \tag{17}$$

where T''_m is the bulk mean temperature at the bottom of the previous upper tube. Dimensionless variables appearing in the above equations are defined as follows:

$$x'' = \bar{x}/s,\ 0 \le x'' \le 1$$

$$y'' = \bar{y}/\delta_s,\ 0 \le y'' \le 1$$

$$S'' = 2S/(\nu^2/g)^{1/3}$$

$$T'' = (T - T_v)/(T_w - T_v) \tag{18}$$

This problem differs from the classical Graetz problem which has been thoroughly described and extended by Drew (1931), Jacob (1949), Kays (1955), and Sellars et al. (1956). The difference is due to the increasing velocity and decreasing film thickness caused by the free fall of the film.

By using the finite difference method, the temperature distribution of the falling liquid sheet between the tubes is numerically solved from Eqs. 16 and 17. The temperature profile at the end of the liquid sheet between two successive tubes is used as the starting temperature profile at the top of the next lower tubes in Eq. 6. It is to be noted that Eq. 14 that is used in the energy equation to predict the temperature distribution within

the film may introduce some numerical difficulties as x approaches zero since it results in an infinite local width $2\,\delta_s$ of the liquid film. However, as long as the grid size, Δx, is not too small, this does not cause any serious problem for the numerical technique described here.

Stagnation point boundary layer solution at the top of the tubes

For liquid falling between tubes, it is assumed that a continuous liquid sheet with a uniform cross sectional velocity which is increasing due to the free fall leads to a two-dimensional liquid jet impinging on the top of the next tube. Since the width of the falling liquid sheet is very thin compared to the tube diameter, the problem may be treated as a jet impinging on a flat surface, Figure 3. Therefore, a velocity, resulting from the stagnation point boundary layer development theory with a uniform velocity profile outside the boundary, is used for the starting velocity profile near the impingement point. One such profile given by Schlichting (1979) for the u-velocity component is

$$u = Cx[(2\eta - 2\eta^3 + \eta^4) + \frac{\Lambda}{6}(\eta - 3\eta^2 + 3\eta^3 - \eta^4)],\ \eta \le 1$$

$$u = Cx,\ \eta > 1 \tag{19}$$

where

$$\eta \equiv y/\delta_b$$

$$\delta_b \equiv (\Lambda\nu/C)^{0.5}, \text{ boundary layer thickness}$$

where

$$\Lambda \equiv (\delta_b^2/\nu)\,(du/dx)$$

The uniform velocity, Cx, at the stagnation point is obtained from the general case of wedge flows. The profile at the stagnation point corresponds to $\Lambda = 7.052$.

For a two-dimensional jet flow with a uniform velocity profile impinging on a flat surface, the numerical values of C have been reported by Sparrow and Lee (1975) and Miyazaki and Silberman (1972) for a two-dimensional jet emerging from a slot. Their results vary with the ratio of the slot height above the impingement surface, S, to the slot width $(2\delta_s)$.

$$\text{At } \frac{S}{2\delta_s} = 1.5, \left(\frac{C}{u_\infty}\delta_s\right)^{1/2} = 0.676 \quad \text{(Sparrow and Lee)}$$

$$\left(\frac{C}{u_\infty}\delta_s\right)^{1/2} = 0.667 \quad \text{(Miyazaki and Silberman)}$$

$$\text{and for } \frac{S}{2\delta_s} \to \infty \left(\frac{C}{u_\infty}\delta_s\right)^{1/2} = 0.627 \quad \text{(Miyazaki and Silberman)} \tag{20}$$

where u_∞ is the impinging jet velocity.

Since liquid descending from one tube to the next lower one is considered as a continuous jet impinging on the top of the tube, Figure 3, the impingement velocity is given by

$$u_\infty = (2gS)^{1/2} \tag{21}$$

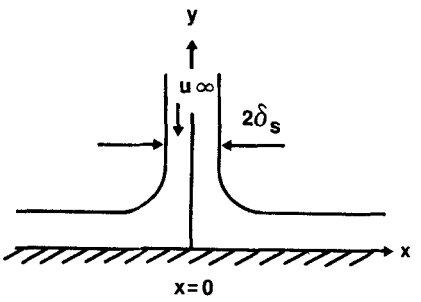

Figure 3. Modeling of jet impinging on a flat surface.

For a liquid mass flow rate 2Γ, the width, $2\delta_s$, of the falling jet just above the top of the tube becomes

$$2\delta_s = \frac{2\Gamma}{\rho u_\infty} \tag{22}$$

For example, water at 100°C with $\Gamma = 0.1$ kg/m · s (Re = 1,413) falling on a tube bundle with $S = 0.0127$ m and $D = 0.0254$ m yields $\delta_S = 0.00021$ m. Since the flow field on the top of the tube can be considered as a jet impinging on a flat surface, the stream velocity gradient near the stagnation point is assumed to be equal to the Miyazaki and Silberman's result (0.627) in Eq. 20 for large values of $S/2\delta_s$. Substitution of Eqs. 21 and 22 into Eq. 20 gives the free stream velocity gradient at the stagnation point $x = 0$ as

$$C = 0.787\,\frac{\rho g S}{\Gamma} \tag{23}$$

In Eq. 25, the boundary layer thickness near $x = 0$ can be obtained as

$$\delta_b = (7.052\nu/C)^{0.5} = 2.116\nu(Re/2gS)^{0.5} \tag{24}$$

Schlichting (1979), Sparrow and Lee (1975) and Miyazaki and Silberman (1972) showed that after impingement, the free stream velocity $u(x)$ increases rapidly from zero at $x = 0$ and becomes finally invariant with the flow direction after $x = 4\delta_s$. Hence, the film thickness at $x_o = 4\delta_b$ can be obtained as

$$\Gamma = \rho\int_0^{\delta_b} u\,dy + \rho\int_{\delta_b}^{\delta_f} Cx_o\,dy = \rho C x_o(\delta_f - 0.2412\delta_b) \tag{25}$$

Thus,

$$(\delta_f)_{x_o} = \Gamma/(\rho C x_o) + 0.2412\delta_b \tag{26}$$

Furthermore, substituting Eqs. 22, 23 and 24 into Eq. 26 gives the ratio of boundary layer thickness to the film thickness as

$$\frac{\delta_b}{\delta_f} = \left(\frac{Re^{1/2}}{13.33} + 0.2412\right)^{-1} \tag{27}$$

which has a value of about 0.2 to 0.4 corresponding to Re ranging from 4,000 to 800, respectively. This result indicates that the boundary layer thickness remains small compared to the remaining inviscid film region.

The stagnation point boundary layer velocity profile of Eq. 19 at $x = 4\delta_s$ is now used as the initial liquid film velocity at the top of the tubes. The initial u-component velocity is then given from Eq. 19 as

$$u_o = C(4\delta_s)[2\eta - 2\eta^3 + \eta^4 + 1.175(\eta - 3\eta^2 + 3\eta^3 - \eta^4)], \eta \le 1$$
$$u_o = C(4\delta_s), \eta > 1 \quad (28)$$

where δ_s and C are given in Eqs. 22 and 23 respectively and the initial v-component velocity may be assumed with negligible error to be equal to zero. The dimensionless initial velocity components of u and v can now be expressed as

$$u'_o = 6.30\frac{S'^{0.5}}{Re}\left[2\frac{u'}{m'} - 2\frac{y'^3}{m'^3} + \frac{y'^4}{m'^4} + 1.175\left(\frac{y'}{m'} - \frac{3y'^2}{m'^2} + \frac{3y'^3}{m'^3} - \frac{y'^4}{m'^4}\right)\right] \quad 0 \le y' \le m' \quad (29)$$

$$u'_o = 6.3\frac{S'^{0.5}}{Re}, m' \le y' \le 1$$
$$v'_o = 0 \quad (30)$$

where $m'(\equiv \delta_b/\delta_f)$ is known from Eq. 27.

By integrating the dimensionless initial u-velocity component (Eq. 29) across the film thickness, the dimensionless film thickness, δ'_o, (Eq. 12) becomes

$$\delta'_o = \left(6.3 - 1.52\frac{\delta_b}{\delta_f}\right)^{-1}\frac{Re}{S'^{0.5}} \quad (31)$$

These are the boundary conditions for the subsequent film flow analysis as described earlier.

Local and averaged heat transfer coefficient

Utilizing boundary conditions (Eqs. 4–6) and starting values for v'_o, u'_o and δ'_o (Eqs. 29–31), Equations 1–3 and 12 can be numerically solved for the local film thickness, velocity, and temperature along the perimeter for $0 < \theta < \pi$.

The local heat transfer coefficient around the tubes is defined as

$$h(\theta) \equiv \frac{\dot{q}''_w}{T_w - T_v} \quad (32)$$

For *constant heat flux*, the local Nusselt number may be expressed in terms of dimensionless temperature at the wall as

$$Nu(\theta) \equiv \frac{h(\theta)L_c}{k} = \frac{1}{T'_w} \quad (33)$$

Alternatively for a *constant wall temperature*, the local heat transfer coefficient and local Nusselt number are given as follows:

$$h(\theta) \equiv \frac{\dot{q}''_w}{T_w - T_v} = \frac{-k}{\delta_f}\left(\frac{\partial T'}{\partial y'}\right)_{y'=0} \quad (34)$$

$$Nu(\theta) = -\frac{1}{\delta'}\left(\frac{\partial T'}{\partial y'}\right)_{y'=0} \quad (35)$$

As discussed earlier, except at very low film Reynolds numbers, liquid films develop an interfacial wave structure, which increases heat transfer rates above those obtained for smooth liquid film flows. The increase in heat transfer is attributable to the presence of interfacial waves which provide a greater heat transfer surface and, more importantly, agitate the liquid film. However, assuming that the effects of waviness will be similar to those on vertical falling films, the theoretical heat transfer coefficient is modified for waviness by using empirical correlation developed by Zazuli (1955) as

$$h(\theta)_{\text{wavy}} = 0.687Re^{0.11}h(\theta)_{\text{laminar}} \quad (36)$$

The application of Zazuli's correlation factor to predicted smooth-film heat transfer coefficients established for laminar films on vertical surfaces to laminar films on horizontal tubes has been successfully used and experimentally confirmed by Moalem and Sideman (1976), Chun and Seban (1971) and Seban (1978). Similar empirical correction of Labuntsov (1957) was used by Kutateladze and Gogonin (1979) and Rogers (1981) although the correction factor in this case is slightly different from the one used here.

The averaged heat transfer coefficient is obtained by integrating the local value of $h(\theta)_{\text{wavy}}$, which yields

$$\bar{h} = \frac{1}{\pi}\int_0^\pi h(\theta)_{\text{wavy}}\, d\theta \quad (37)$$

Thus, the average Nusselt number may be given by $\bar{Nu} = \bar{h}L_c/k$.

After evaluating the heat transfer coefficient at the topmost tube, the local flow rate Γ and temperature profile reaching the top of the next lower tube are solved from Eqs. 15 and 16, respectively. The heat transfer coefficient for this tube is determined with the same finite difference scheme by solving the film thickness and temperature profile for a film flowing over a heated tube. By using the local flow rate and temperature profile reaching a given tube, the heat transfer coefficients of each lower tube is determined successively in a same manner as discussed above. The heat transfer coefficient for the entire tube bank then becomes the arithmetic average of the heat transfer coefficients of all the individual tubes.

The top tube is found to have the highest coefficient. This decreases progressively with subsequent tubes due to the thermal boundary layer development. When the calculated heat transfer coefficients for two successive tubes only differs by a small tolerance, this may be considered as thermally developed flow, and, thus, the same heat transfer coefficients are used for all lower tubes. Although the liquid flow rates in the thermally developed region are slightly decreased, this does not significantly affect the heat transfer coefficients as long as all tubes remain fully wetted.

Results and Discussion

The present study represents an attempt to predict the local and average values of the heat transfer coefficients on a single heated tube, as well as on any evaporator tube in a multiple tube

bank. Solutions are obtained numerically to examine the characteristics of the basic variables affecting the heat transfer coefficients. The numerical results are compared with available experimental data and are discused in terms of the parameters involved.

Figure 4 shows the variation of predicted film thickness with the inclination angle around a horizontal tube for various film Reynolds numbers. For higher flow rates, the film thickness is greatest at the top of the tube, whereas for smaller flow rates the film thickness is thicker at the bottom of the tube. Here viscous effects, which result in reducing the film velocity, becomes more significant for a thin film caused by small flow rates. However, for higher flow rates, the viscous effects on the film flow are less than the effects of gravity which accelerates the film flow and thus reduces the film thickness. Figure 4 also compares the film thicknesses obtained by the Nusselt solution, which neglects inertia forces, at various flow rates. As expected, at small flow rates (Re = 200) the present numerical solution is almost the same as the Nusselt solution, while at increasing flow rates the numerical solution gradually departs from the Nusselt solution. This indicates that inertia effects are important and cannot be ignored at higher flow rates which are typical of the operating range of horizontal tube evaporators ($Re > 800$.)

Figure 5 presents the variation of the film thickness at $\theta = 90°$ with film Reynolds number for various Prandtl numbers and vertical tube spacings. These results are compared with the measured film thickness data of Solan and Zfati (1974) at $Pr = 5$. The film thickness increases with increasing Prandtl number and with decreasing vertical tube spacing. This is due to the fact that increasing the Prandtl number increases viscous forces and decreasing the vertical tube spacing decreases the initial film velocity. As observed in Figure 5, as the film Reynolds number decreases, the film thickness also decreases. The effect of vertical tube spacing, illustrated for $Pr = 5$, is reduced at lower Re by having the viscous force acting on a thinner film. This behavior was observed by Mitrovic (1986). The experimental data of

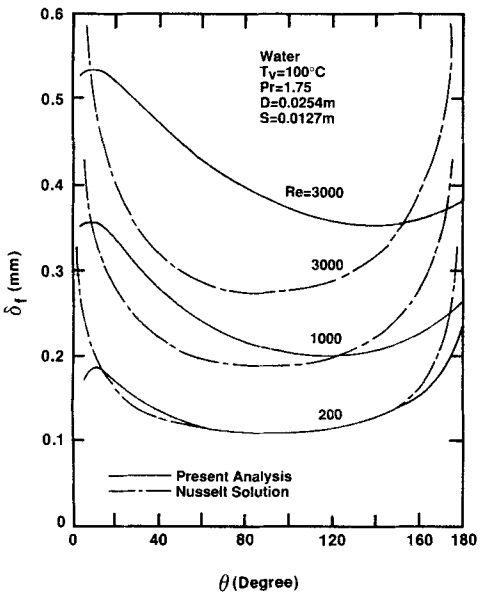

Figure 4. Predicted film thickness around a horizontal tube.

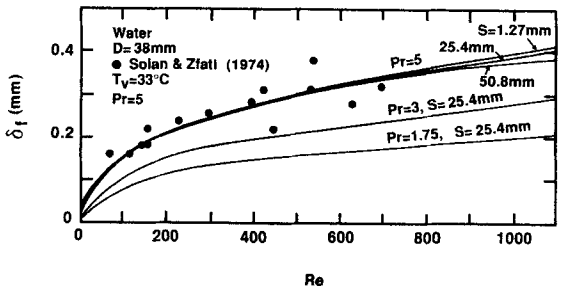

Figure 5. Comparison of predicted film thickness at θ = 90° with Solan and Zfati's Data (1974).

Solan and Zfati (1974) scatter around the corresponding predicted line with Pr = 5. The scattering increases with increasing film Reynolds number, probably due to the difficulty of experimentally determining the film thickness in wavy flow.

Figures 6 to 8 present the comparison between the calculated circumferential heat transfer coefficients and the experimental measurements of Liu (1975) and Fletcher et al. (1973). The figures show good agreement of the numerical predictions with the experimental results. $h(\theta)$ is largest at the top of the tube and decreases with increasing angle and finally reaches its lowest value at the bottom of the tube. The overprediction near the top of the tube may be attributed to experimental problems of measuring heat transfer coefficients as $x \rightarrow 0$ due to lateral conduction and as well as to the fact that the model does not adequately reflect the physical situation at the location. The underestimation near the bottom of the tubes may be due to the model which leads to thick film while experiments show slight breaking. However, these discrepancies between the theoretical and experimental results does not greatly affect the average heat transfer coefficient over the circumferential length of the tube and the present local prediction.

Figure 6, with numerical results for q'' = 27,560 to 67,600 W/m^2, shows that the heat flux has no effect on the heat transfer coefficient. There is some scatter of Liu's data which was reported as being due to the instability of the flow conditions. The local heat transfer coefficient increases with increasing

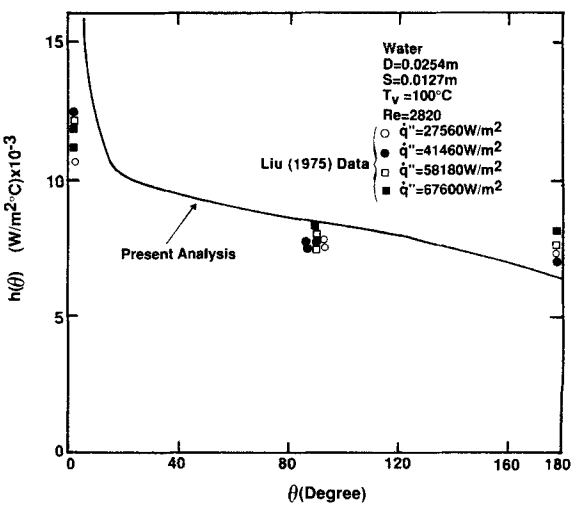

Figure 6. Effect of heat flux on the local heat transfer coefficient.

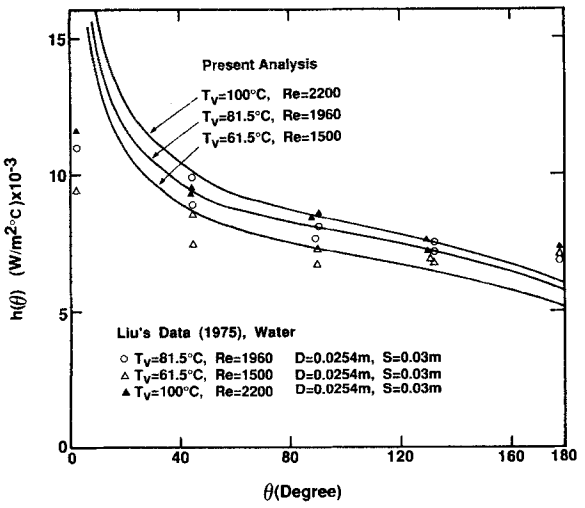

Figure 7. Effect of saturation temperature on the local heat transfer coefficient and comparison with experimental data.

saturation temperature and decreasing tube diameter as shown in Figures 7 and 8. This effect is due to the decreasing liquid viscosity with the increasing temperature. Figure 8 also shows the effect of pipe diameter for the same flow conditions. The local heat transfer coefficient at same θ decreases with increasing pipe diameter. This is not surprising because as θ increases thermal boundary layer increases more rapidly on larger diameter pipe than the smaller one resulting in higher heat transfer coefficients for smaller pipe than the larger pipe.

The comparison of the predicted average heat transfer results with the reported averaged heat transfer data for film evaporation on a horizontal tube are shown in Figures 9 to 13. Figure 9 shows the effect of vertical tube spacing on the averaged heat transfer coefficient. Here Nu increases slightly with increasing S. The present predictions agree remarkably well with the experimental observations of Liu (1975) and Chyu and Bergles (1987).

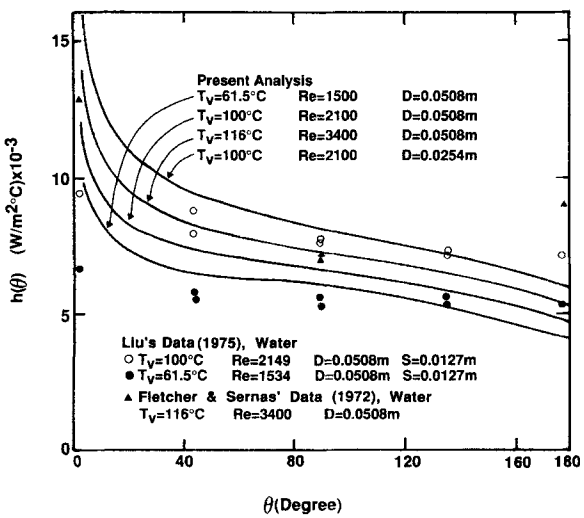

Figure 8. Effect of saturation temperature and tube diameter on the local heat transfer coefficients and comparison with experimental data.

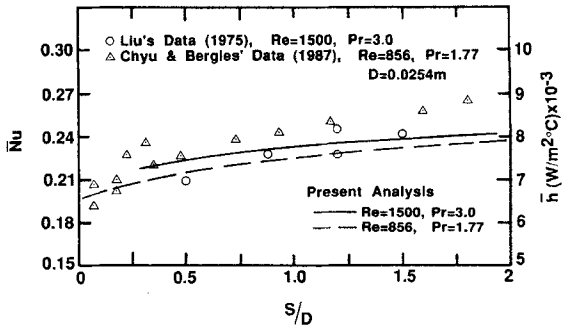

Figure 9. Effect of vertical tube spacing on the average heat transfer coefficient and comparison with experimental data.

A comparison of present predictions with the data of Fletcher and Sernas (1972), Liu (1975), Chyu and Bergles (1987) and the correlations of Chun and Seban (1971), Sernas (1979) and Lorenz and Yung (1972) is shown in Figure 10 for 2.54 cm diameter tube. The calculated results and Lorenz and Yung's correlation give a good agreement with the experimental data. Chun and Seban's correlation consistently under predicts the heat transfer coefficient. This is not surprising since their correlation was based on the vertical tube data and the classical Nusselt solution where thermal development was neglected. Sernas' correlation, which is based on Parken's data (1975), also gives a lower prediction, probably due to the reduced waviness of Parken's data. The liquid film flow of Parken's test carefully deposited the liquid film on the top of the tube through a small falling distance (3 mm) such that laminar flow was obtained in his test with *Re* as high as 6,000.

Figure 11 compares the present predictions with the ammonia data of Owens (1978) and Conti (1978). For Re < 1,500, the predictions are substantially below the ammonia data. Since considerable scattering exists in the ammonia data, especially at small Re, additional experimental tests are necessary to correctly verify the present analysis for relatively low *Re*. More importantly this figure illustrates the relative effects of Peclet number as expected from the dimensionless form of the energy equation, Eq. 3. Noting that the Peclet number is the ratio of two heat transfer modes, that of convection to that of conduction, the conduction is important at low *Re* numbers ranges

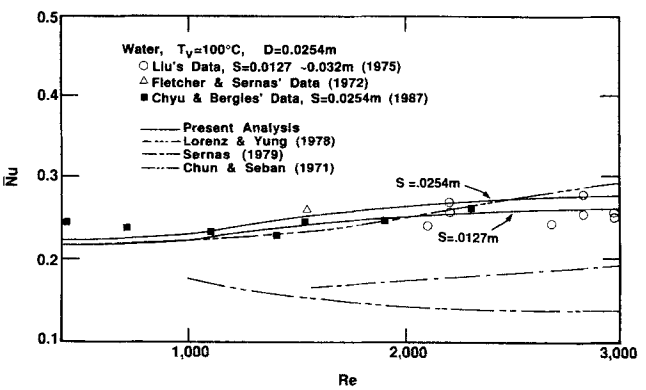

Figure 10. Effect of Reynolds number on the average heat transfer coefficient and comparison with experimental data.

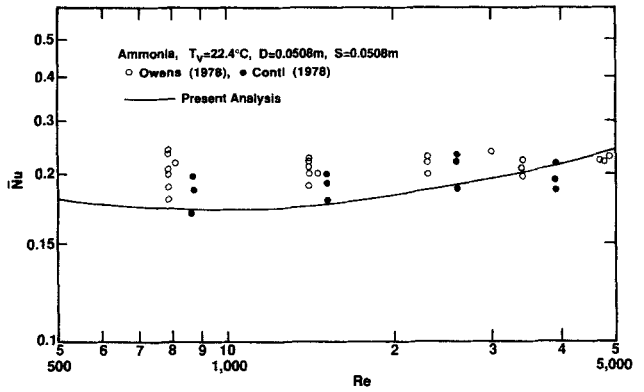

Figure 11. Comparison of present predictions with Owens (1978) and Conti's (1978) ammonia data.

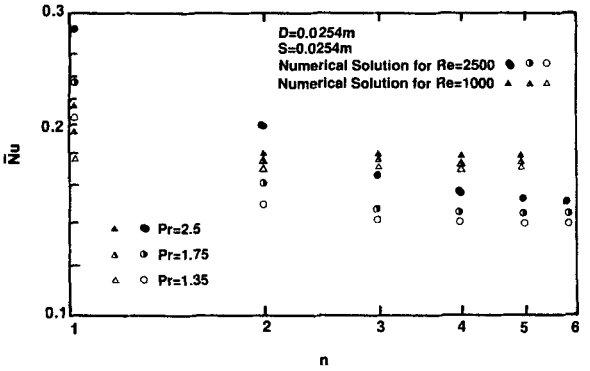

Figure 13. Variation of Nusselt number with tube number in a horizontal tube bundle.

resulting in decreasing *Nu* as *Re* increases for a given *Pr* number. However, as *Re* increases the convective heat transfer gradually overcomes the opposing effects of the conduction heat transfer, and causes a *Nu* behavior change as verified by the figure. Traditionally this behavior change has been attributed to flow regime transition from laminar to turbulent. As evident from this figure and from Figure 14 presented later, the heat transfer performance can be affected by the convective heat transfer mode even in the laminar flow regime as the Peclet number increases.

Figure 12 presents the predicted average heat transfer coefficient with the data of Liu (1975) and the nonnucleate boiling data of Fletcher et al. (1972). Most of the data has a maximum discrepancy of ±20% with the predictions; the mean deviation is about 10.3%. The overall agreement with experimental results over a very wide range of parameters indicates that the principle mechanisms involved are properly accounted for by the present model.

Figure 13 presents the prediction of heat transfer variations within a tube bundle for two different flow rates. It shows that the top tube has the highest Nusselt number and the tube average Nusselt number decreases for subsequent tubes until the thermally developed region is reached. For further tubes heat transfer coefficients are constant. This behavior is due to the development of liquid temperature profile as the liquid falling along the tube bundle. This heat transfer trend is analogous to the liquid flow in tubes where the heat transfer coefficient is higher in the thermally developing region near the tube inlet and reduces to a fully developed value further downstream. Figure 13 also shows that the thermally developed region is more easily attained for a small flow rate because of its relatively thin film thicknesses.

Figure 14 attempts to compare the present thermally developed results for constant heat flux with the thermally developed data of Chun and Seban's (1971) vertical tube test. Since there is no data available in the open literature for the case presented here, a comparison is made with Chun and Seban's correlation which was based on vertical wall experiments. It is seen that the heat transfer characteristics for the film flows over the horizontal and vertical tubes are similar. However, the vertical tube data are higher than the present thermally developed prediction for horizontal tubes since the greater accelerational force (g for vertical tubes and $g \sin\theta$ for horizontal tubes) acted on the liqid film flow along the vertical tubes results in a thinner film thickness and higher heat transfer coefficient. Furthermore, Figure 14 shows the opposing effects of convective and conductive heat transfer as scaled by the Peclet number, $Pe \equiv Re \cdot Pr$. As commented with respect to Figure 11, the convective heat transfer overcomes the adverse effect of conductive heat transfer as Reynolds number increases for a given value of Prandtl number.

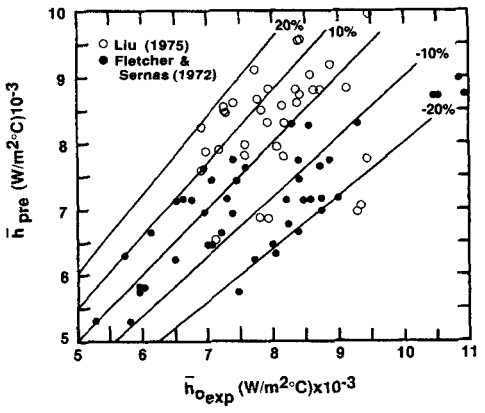

Figure 12. Comparison of predicted average heat transfer coefficients with experimental data of Liu (1975) and Fletcher (1972).

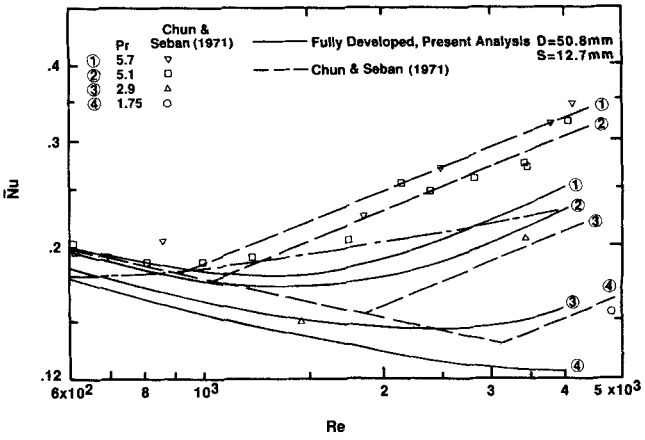

Figure 14. Comparison of the present constant heat flux predictions for a tube bundle with Chun and Seban's results (1971).

This behavior may be in contrast with traditional Nusselt type of solutions where it was assumed that heat is transferred through conduction across the liquid film. Again, as commented with respect to Figure 11, the heat transfer performance of film flow on horizontal tubes can be affected by the convective heat transfer mode even in the laminar flow region as the Peclet number increases. The predictive results illustrated here are in full agreement with those presented by Dukler (1960) and with Liu's (1975) experimental observations.

As may be noted from the figures, the predictions of the film thickness and of local and average heat transfer coefficients of film flowing over horizontal tubes are in good agreement with the reported experimental data for the operating ranges of typical horizontal tube evaporators. They also predict heat transfer behavior which is similar to that of the fully developed data for vertical tubes. Further studies have been undertaken to investigate the effects of constant heat flux and constant temperature boundary conditions. The average heat transfer coefficient obtained for constant heat flux is about 11% higher than that for the isothermal case at the Reynolds number of 2,800. This difference may be attributed to the slightly different shape of the generalized temperature profile near the tube wall surface as explained by Kays (1978).

Summary and Conclusions

An analysis has been presented for the heat transfer predictions of film evaporation on a bank of horizontal tubes which simulates liquid falling on a tube bundle of horizontal tube evaporators. Liquid falling from one tube to the next lower tube is considered as a thin liquid sheet with a uniform free falling velocity impinging on the top of the tube. The velocity profile near the impinging point was obtained from the stagnation point boundary layer theory. Hydrodynamic and heat transfer solutions along each tube were then obtained by a finite difference method. The values of laminar heat transfer coefficient were modified empirically to account for waviness. The analysis took into account the effects of liquid flow rate, saturation temperature level, between-tube distance and was performed for both constant heat flux and isothermal conditions. The variation of average heat transfer coefficient with tube location in a tube bank was also evaluated. It was found that the heat transfer coefficient for the tubes in the bank decreases from the first tube until a fully developed region is reached.

Comparison of the predicted circumferential and average heat transfer coefficients indicated good agreement with the reported data for heated horizontal tubes and a heat transfer behavior similar to that of fully developed data of vertical tubes. The proposed model can, therefore, be safely used for predicting the heat transfer coefficients for liquid film evaporation on the tubes of horizontal evaporators.

Notation

D = diameter
g = gravitational acceleration
$h(\theta)$ = local heat transfer coefficient
h = average heat transfer coefficient
h_{fg} = latent heat of phase change
k = thermal conductivity
L_c = film characteristic length, $(\nu^2/g)^{1/3}$
n = tube number in a tube bank
Nu = Nusselt number
Pe = Peclet numbers, $(Re\ Pr)$
Pr = Prandtl number
q''_w = heat flux
R = radius
Re = Reynolds number, $4\Gamma/\mu$
S = vertical tube spacing
T = temperature
T_m = bulk mean temperature at the bottom of the tubes
T_v = saturation temperature
T_w = wall temperature
u = x-component velocity
u_o = initial velocity at the top of the tubes
u_s, u_∞ = liquid free falling velocities, Eqs. 13 and 21
u_f = film characteristic velocity, Eq. 9
v = y-component velocity
v_o = initial velocity at the top of the tubes
x = tangential coordinate for film flow over horizontal tubes
y = radial coordinate for film flow over horizontal tubes
$\bar{x}$ = vertical coordinate for film falling between tubes
$\bar{y}$ = horizontal coordinate for film falling between tubes

Greek letters

α = thermal diffusivity
δ_f = film thickness
δ_b = boundary layer thickness
θ = peripheral angle
ν = kinematic viscosity
ρ = density
η = dimensionless quantity defined by y/δ_b
Γ = mass flow rate per unit length

Superscripts

$'$ = dimensionless variables for film flow over horizontal tubes
$''$ = dimensionless variables for free falling film between tubes

Literature Cited

Chen, I. Y., "Heat Transfer Analysis of a Falling-Film Horizontal Tube Evaporator," PhD Thesis, Univ. of Wisconsin, Milwaukee, WI (1984).

Chun, K. R., and R. A. Seban, "Heat Transfer to Evaporating Liquid Films," *J. Heat Trans.*, **91c**, 391 (1971).

Chyu, M. C., and A. E. Bergles, "An Analytical and Experimental Study of Falling-Film Evaporation on a Horizontal Tube," *ASME J. of Heat Transf.*, **109**, 983 (1987).

Conti, R. J., "Experimental Investigation of Horizontal-Tube Ammonia Film Evaporators with Small Temperature Differentials," *Proc. Ocean Therm. Ener. Conv. Conf.*, Miami Beach (1978).

Danilova, G. N., V. G. Burkin, and V. A. Dyundin, "Heat Transfer in Spray-Type Refrigerators," *Heat Trans. Soviet Res.*, **8**(6), 105 (1976).

Dhir, V. K., and K. Taghavi-Tafreshi, "Hydrodynamic Transition During Dripping of a Liquid from Underside of a Horizontal Tube," ASME, Paper No. 81-WA/HT-12 (1981).

Drew, T. B., "Mathematical Attacks of Forced Convection Problems: A Review," *Trans. AIChE*, **26**, 26 (1931).

Dukler, A. E., "Fluid Mechanics and Heat Transfer in Vertical Falling Film Systems," *AIChE Symp. Ser.*, **56**(30), 1 (1960).

Fletcher, L. S., and V. Sernas, "Boiling Heat Transfer Coefficients for Thin Water Films in Horizontal Tube Desalination Units," Rutgers Univ., New Jersey Report No. RU-TR 139-MAE-H (1972).

Fletcher, L. S., V. Sernas, and L. S. Galowin, "Evaporation from Thin Water Films on Horizontal Tubes," ASME Paper No. 73-HT-42, ASME/AIChE Heat Transf. Conf., Atlanta (1973).

Fletcher, L. S., V. Sernas, and W. H. Parken, "Evaporation Heat Transfer Coefficients for Thin Sea Water Films on Horizontal Tubes," *Ind. Eng. Chem., Process Design. Dev.*, **14**(4), 411 (1975).

Fujita, T., and T. Veda, "Heat Transfer to Falling Liquid Films and Film Breakdown: I. Subcooled Liquid Film," *Int. J. Heat Mass Transf.*, **21**, 97 (1978).

Ganic, E. N., and M. N. Roppo, "An Experimental Study of Falling Liquid Film Breakdown on a Horizontal Cylinder During Heat Transfer," *J. Heat Transf.*, **102**, 324 (1980).

Inada, S., Y. Miyazaki, and R. Izumi, "A Study on the Laminar-Flow

Heat Transfer Between a Two-Dimensional Water Jet and a Flat Surface with Constant Heat Flux," Bulleting of the JSME, **24**(196), 1803 (1981).
Jacob, M., *Heat Transfer,* **1,** New York (1949).
Kays, W. M., "Numerical Solutions for Laminar Flow Heat Transfer in Circular Tubes," *Trans. ASME,* **77,** 1265 (1955).
Kays, W. M., and M. E. Crawford, *Convective Heat and Mass Transfer,* 2nd ed., McGraw-Hill, New York (1978).
Kocamustafaogullari, G., "Two-Fluid Modeling in Analyzing the Interfacial Stability Liquid Film Flows," *Int. J. Multiphase Flow,* **11,** 63 (1985).
Kutateladze, S. S., and I. I. Gogonin, "Heat-Transfer in Film Condensation of Slowly Moving Vapor," *Int. J. Heat Mass Transf.,* **22,** 1593 (1979).
Labuntsov, D. A., "Heat Transfer in Film Condensation of Pure Vapors on Vertical Surfaces and Horizontal Tubes," *Toploenergetika,* **7,** 72 (1957).
Lipsett, A. W., and R. R. Gilpin, "Laminar Jet Impingement Heat Transfer Including the Effects of Melting," *Int. J. Heat Mass Transf.,* **21,** 25 (1978).
Liu, P., "The Evaporating Falling-Film on Horizontal Tubes," Ph.D., Thesis, Univ. of Wisconsin, Madison, WI (Aug., 1975).
Lorenz, J. J., and D. Yung, "Combined Boiling and Evaporation of Liquid Films on Horizontal Tubes," *Proc. Ocean Therm. Ener. Conv. Conf.,* Miami Beach (1978).
———, "A Note on Combined Boiling and Evaporation of Liquid Films on Horizontal Tubes," *J. Heat Transf.,* **101,** 178 (1979).
Mitrovic, J., "Influence of Tube Spacing and Flow Rate on Heat Transfers from a Horizontal Tube to a Falling Liquid Film," *Proc. Int. Heat Transf. Conf.,* San Francisco, **4,** 1949 (1986).
Miyazaki, H., and E. Silberman, "Flow and Heat Transfer on a Flat Plate Normal to a Two-Dimensional Laminar Jet Issuing from a Nozzle of Finite Height," *Int. J. Heat Mass Transf.,* **15,** 2097 (1972).
Moalem, D., and S. Sideman, "Theoretical Analysis of a Horizontal Condenser-Evaporator Elliptical Tube," *J. of Heat Transf.,* **97,** 352 (Aug., 1975).
———, "Theoretical Analysis of a Horizontal Condenser-Evaporator Tube," *Int. J. Heat Mass Transf.,* **19,** 259 (1976).
Moalem, D., S. Sideman, and H. Horn. "Enhanced Film Mass Transfer Coefficients on Grooved Horizontal Conduits," *Chem. Eng. Sci.,* **34,** 420 (1979).
Moalem, D., S. Sideman, and A. E. Dukler, "Dripping Characteristics in a Horizontal Tube Evaporator," *Desalination,* **27,** 117 (1978).
Newson, I. H., "Heat Transfer Characteristics of Horizontal Tube Multiple Effect Evaporators—Possible Enhanced Tube Profiles," *Proc. Int. Symp. Fresh Water from the Sea,* **2,** 113 (1978).
Owens, W. L., "Correlation of Thin Film Evaporation Heat Transfer Coefficients for Horizontal Tubes," *Proc. Ocean Therm. Ener. Conv. Conf.,* Miami Beach (1978).
Parken, Jr., W. H., "Heat Transfer to Thin Water Films on Horizontal Tubes," Ph.D. Thesis, Rutgers Univ. (June, 1975).
Parken, Jr., W. H., and L. S. Fletcher, "Heat Transfer in Thin Liquid Films Flowing over Horizontal Tubes," *Proc. Int. Heat Transf. Conf.,* **4,** München, Germany (Sept., 1982).
Rogers, J. T., "Laminar Falling-Film Flow and Heat Transfer Characteristics on Horizontal Tubes," *Can. J. of Chem. Eng.,* **59,** 213 (Apr., 1981).
Sabin, C. M., and H. F. Poppendiek, "Film Evaporation of Ammonia over Horizontal Tubes," *Proc. Ocean Ther. Ener. Conv.,* Miami Beach (1978).
Schlichting, H., *Boundary-Layer Theory,* 7th ed., McGraw-Hill, New York (1960).
Seban, R. A., "Transport to Falling-Films," Keynote Paper KS-30, *Proc. Int. Heat Transf. Conf.,* **6,** 417, Toronto, Canada (Aug., 1978).
Sellars, J. R., M. Tribus, and J. S. Klein, "Heat Transfer to Laminar Flows in a Round Conduit: The Graetz Problem Extended," *Trans. ASME,* **78,** 441 (1956).
Sernas, V., "Heat Transfer Correlation for Subcooled Water Films on Horizontal Tubes," *J. Heat Transf.,* **101,** 176 (1979).
Sideman, S., H. Horn, and D. Moalem, "Transport Characteristics of Films Flowing Over Horizontal Smooth Tubes," *Int. J. Heat Mass Transf.,* **21,** 285 (1978).
Sideman, S., and D. Moalem, "Performance Improvement of Horizontal Evaporator-Condenser Desalination Units," *Proc. Int. Symp. of Fresh Water from the Sea,* **2,** 315 (1976).
Solan, A., and A. Zfati, "Heat Transfer in a Laminar Flow of a Liquid Film on a Horizontal Cylinder," *Proc. Int. Heat Transf., Conf.,* Paper FC 2.9, 90, Tokyo, Japan (1974).
Sparrow, E. M., and L. Lee, "Analysis of Flow Field and Impingement Heat/Mass Transfer Due to a Nonuniform Slot Jet," *J. Heat Transf.,* **97,** 191 (1975).
Universal Desalting Corp., "Pilot Plant Tests and Design Study of a 2.5 MGD Horizontal Tube Multiple-Effect Plant," Office of Saline Water, Report No. 492 (Oct., 1969).
———, "Second Report on Horizontal-Tube Multiple-Effect Process Pilot Plant Tests and Design," Office of Saline Water, Report No. 592 (May, 1970).
———, "Third Report on Horizontal-Tube Multiple-Effect Process Pilot Plant Tests," Office of Saline Water, Report No. 740 (Oct., 1971).
———, "Fourth Report on Horizontal-Tube Multiple-Effect Process Pilot Plant Tests," Office of Saline Water, Report No. 967 (July, 1972).
———, "Fifth Report on Horizontal-Tube Multiple-Effect Process Pilot Plant Tests," Office of Saline Water, Report No. 963 (Dec., 1972).
Weda, T., and H. Tanaka, "Measurement of Velocity, Temperature and Velocity Fluctuation Distributions in Falling Liquid Films," *Int. J. Multiphase Flow,* **2,** 261 (1975).
Yung, D., J. J. Lorenz, and E. N. Ganic, "Vapor/Liquid Interaction and Entrainment in Falling Film Evaporators," *J. Heat Transf.,* **102,** 20 (1980).
Zazuli, N. V., "Investigation of Heat Transfer with Vapor Condensation in Vertical Tubes," *Heat Transfer and Thermal Modelling* (in Russian), *Izd. Akad. Nauk SSSR,* 278, Moscow (1959).

Manuscript received Aug. 24, 1987, and revision received Apr. 11, 1988.